

Development and on orbit test of Taiji-1 inertial reference

Zhi Wang^{*,†,‡,§} and Jun-Gang Lei^{§,||}

^{*}Changchun Institute of Optics, Fine Mechanics and Physics, CAS, Changchun 130033, China

[†]Taiji Laboratory for Gravitational Wave Universe (Beijing/Hangzhou),
University of Chinese Academy of Sciences (UCAS), Beijing 100049, China

[‡]School of Fundamental Physics and Mathematical Sciences,
Hangzhou Institute for Advanced Study, UCAS, Hangzhou 310024, China

[§]Lanzhou Institute of Physics, Lanzhou 730000, China

^{||}wz070611@126.com

^{||}Lei7412@163.com

^{**}On behalf of The Taiji Scientific Collaboration

Received 15 September 2020

Accepted 30 October 2020

Published 10 March 2021

Taiji-1 is the first step of China's efforts on the detection of gravitational waves in space. It is a one-year quick mission, which aims to verify the key technologies on orbit. The detection of gravitational waves at mHz frequency band needs to exceptionally focus on small spatial deviations between two inertial references several million kilometers apart. The inertial reference on **Taiji-1** spacecraft (S/C) has been developed based on a capacitive readout and actuation scheme to meet the requirements of accelerometer. In this paper, the development condition, ground tests and on-orbit performance of this inertial reference are described.

Keywords: Gravitational waves detection in space; **Taiji** program; inertial reference.

1. Introduction

The detection of gravitational waves at mHz frequency band requires an initial reference for the spaceborne drag-free control system with unprecedented residual acceleration and a laser-interferometer system that is able to detect exceptionally small spatial deviations between two reference sensors several million kilometers apart. The test mass (TM), used as the reflecting mirror of such a gravitational wave detector, is the inertial reference. The sensor electronics is the electronic system required to sense the position of the TM in the spacecraft (S/C) and to actuate it in all degrees of freedom, except in the measurement axis used for gravitational wave detection.^{1,2}

^{||}Corresponding authors.

^{**}For more details, please refer to article 2102002 of this Special Issue.

Taiji program is a space mission launched by Chinese Academy of Sciences.^{3,4} It was designed to measure gravitational radiation over a broad band of low frequencies from about 1 mHz to 1 Hz, where the universe is richly populated by strong sources of gravitational waves.⁵ **Taiji** program will be completely launched in 2030s in three steps. As the first step, **Taiji-1** was launched successfully on 31 August, 2019, aiming to verify the key technologies (such as laser metrology and inertial reference) on one S/C.

2. Taiji-1 — The First Step of China's Efforts

The successful and quick mission Taiji-1 was approved on 30th August 2018 and is planned to fly on 31st August 2019. The Taiji-1 S/C weights 180 kg. The orbit of Taiji-1 is a 97.69° circular sun-synchronous dawn/dusk orbit. The orbit has a relatively stable sun-facing angle, which ensures that the batteries can always be properly charged and that the temperature inside the S/C shall not fluctuate too much. To save the launching cost, the orbital altitude was chosen to be 600 km. Similar to LISA Pathfinder,⁶ Taiji-1 S/C also witnessed the onboard testing of two major technology units, namely laser metrology system⁷ and inertial reference system.¹ Due to short development period and limited budget, the payload design was highly simplified. The laser metrology system consists of an optical bench, a phasemeter and two laser sources, while the inertial reference system is composed of an initial sensor, a drag-free controller and two types of micro-propulsion systems. The distribution of payloads on the Taiji-1 S/C is shown in Fig. 1.

The inertial reference on Taiji-1 S/C works as an accelerometer.⁸ It is composed of sensor and electronics. The sensor consists of an electrode housing and a TM (see Fig. 2(c)). The inertial reference has three axes, including one nonsensitive axis and two sensitive axes (Fig. 2(c)). The nonsensitive axis is Earth-pointing and drag-free. The first

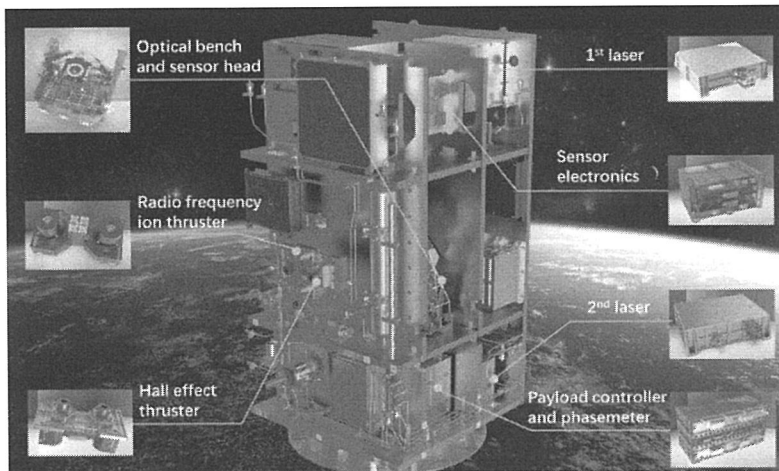


Fig. 1. Taiji-1 S/C and its payloads.

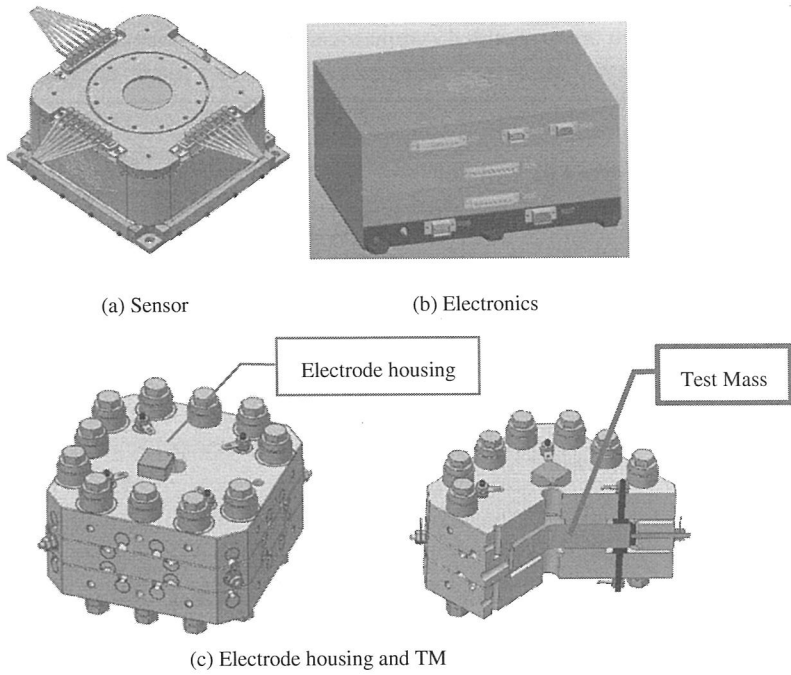


Fig. 2. Inertial reference

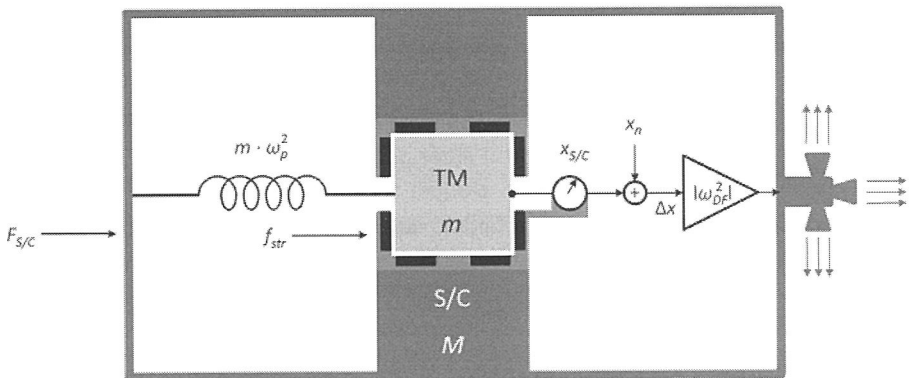


Fig. 3. On-orbit function diagram of inertial reference.

sensitive axis is along the flight direction. With the technique of capacitive sensing, the sensor measured the disturbing acceleration of Taiji-1 S/C. The data was sent to a drag-free controller. Then the controller instructed the thruster to exert forces to compensate for the disturbing force on Taiji-1 S/C. Two different types of thrusters (radio-frequency

ion thruster and Hall Effect thruster) were tested. There are four individual thrusters in each type, which are assembled symmetrically on both sides of the satellite (see Fig. 1). The two types of thrusters, like the two lasers, serve as the backup for each other.

3. Initial Reference of Taiji-1

The TM (whose mass is m) surrounded by sensing electrodes and protected by the S/C (whose mass is M) is affected by a spring-like position-dependent coupling ω_p between TM and S/C and by a position-independent internal stray force f_{str} . The reader uses the position noise to measure the position of S/C relative to TM, denoted as x_n , which is minimized by the drag-free controller forcing the precision thrusters to follow the free-falling TM and to counteract the external forces on S/C.⁹

3.1. Design constraints

According to the orbit frequency and the measured data of the nonconservative force of GRACE satellite at 450 km orbit altitude,¹⁰ the peak value of nonconservative force is 3×10^{-7} m/s in the flight direction and $10^{-8} \sim 10^{-7}$ m/s² in radial and lateral directions. Therefore, in the measurement mode, the range of inertial reference must reach the level of 10^{-6} m/s². Considering the design margin, the range of Taiji-1 inertial reference has been designed to be 3×10^{-5} m/s².

The temperature fluctuation inside the Taiji-1 S/C will affect the structural parameters of the sensor and the circuit parameters of the electronics and then cause the fluctuation of deviation value. Considering the temperature environment inside the S/C, the GRS has been installed in the Taiji-1 S/C (see Fig. 1) by referring to the temperature control index 0.1°C/orbit of Super STAR accelerometer on GRACE. In addition, the Taiji-1 S/C provides the temperature stability of $\pm 0.1^\circ\text{C}$ at sensor and $\pm 0.5^\circ\text{C}$ at electronics.

3.2. Design requirements

According to the requirements of Taiji-1 satellite engineering mission, the technical requirements of Taiji-1 inertial reference and the comparison between Taiji-1 and Taiji-3 inertial references are shown in Table 1.

Table 1. Key requirements of Taiji-1 GRS versus key requirements of Taiji-3.

Parameter	Taiji-3	Taiji-1
Range	1×10^{-9} m/s ²	3×10^{-5} m/s ²
Bandwidth	1 mHz–1 Hz	10 mHz–1 Hz
Position noise	1.8 nm/Hz ^{1/2}	1 nm/Hz ^{1/2}
Actuation noise	$\leq 2 \times 10^{-6}$ V/Hz ^{1/2}	$\leq 2 \times 10^{-5}$ V/Hz ^{1/2}
Readout noise	$\leq 5 \times 10^{-6}$ V/Hz ^{1/2}	$\leq 2 \times 10^{-5}$ V/Hz ^{1/2}
Acceleration noise	3×10^{-15} m/s ² /Hz ^{1/2}	3×10^{-9} m/s ² /Hz ^{1/2}

Table 2. Design parameters of Taiji-1 inertial reference.

	Parameter	Value	Unit
Sensor	Mass of the TM, m	72	g
	Average electrode distance on Y, Z-axis, dy, dz	75	μm
	Average electrode distance on X-axis, dx	60	μm
	Electrode area on Y, Z-axis, SY, SZ	2	cm^2
	Electrode area on X-axis, SX	10	cm^2
Electronics	Bias voltage, VP	5	V
	Effective value of sensing voltage, Vd	4	Vrms
	Sensing voltage frequency, fd	100 k	Hz
	Maximum feedback voltage, Vf	± 10	V

The design parameters of the sensor and electronics are shown in Table 2.

3.3. System composition and working principle

The Taiji-1 inertial reference is composed of a sensor and its electronics, as shown in Fig. 4. As mentioned above, Taiji-1 inertial reference is based on the development basis of accelerometer. In order to support the ground test, a high-voltage suspension module has been designed. The sensor is used to measure the input acceleration signal and output the differential capacitance displacement measurement signal. It is mainly composed of a sensitive structure, a mounting base and a sealing structure. The electronics is used to sense, process and calculate the differential capacitance signal input by the sensor and then output the corresponding actuating voltage signal to the sensor to keep TM at the center of the electrode housing, so as to realize the measurement of Taiji-1 acceleration signal. The electronics consists of a three-axis (X, Y, Z) six-channel differential capacitance sensing circuit, a PID servo feedback control circuit, an actuating circuit and a scientific-data acquisition circuit. At the same time, Taiji-1 inertial reference needs to be designed with a vacuum maintenance module and a high-voltage suspension circuit module in order to meet the requirements of ground test.

In order to realize high-precision capacitance difference sensing, the TM is connected with electronics through a $20\ \mu\text{m}$ gold wire to apply an AC excitation signal. The working principle of Taiji-1 inertial reference, as shown in Fig. 6, is based on the measurement of an electrostatic force required to keep TM at the center of the electrode housing. As a common electrode, the TM, together with the surrounding electrodes, forms a capacitance bridge, which applies the AC modulation sensing voltage signal V_d and the DC bias voltage signal V_p to TM through the gold wire. When an external nonconservative force acts on Taiji-1 S/C, the TM, as the inertial reference, will change its position relative to the surrounding electrodes and deviate from the center of the electrode housing to generate a differential capacitance signal. After being sensed by the sensing circuit and adjusted by PID controller, this signal turns into the feedback voltage signal V_f that is applied to the electrode through the actuating circuit and is proportional

to the input acceleration. This voltage reflects the magnitude of the acceleration input from outside.

When the Taiji-1 inertial reference works as an accelerometer and the TM is stably controlled at the center of the electrode housing, the feedback control output will be linearly related to the input:

$$a_{out} = a_e \cong \frac{2\varepsilon_0\varepsilon_r S}{md^2} V_p V_f, \tag{1}$$

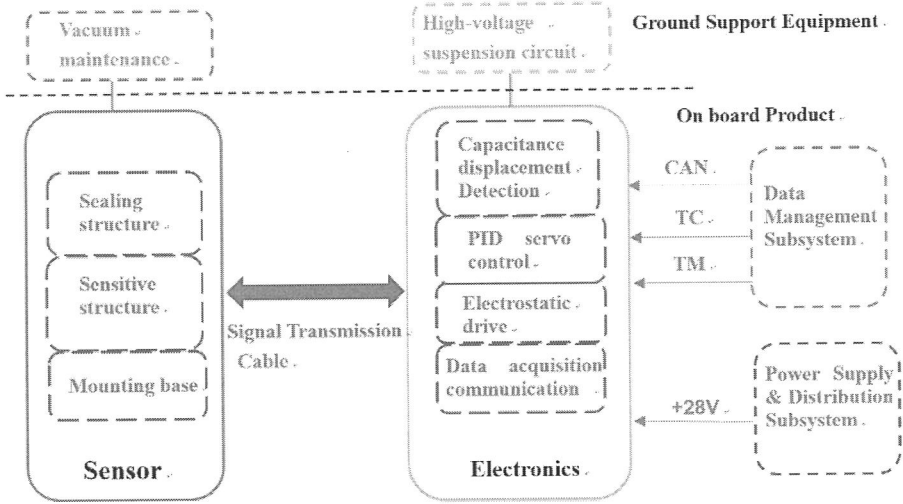


Fig. 4. Composition of Taiji-1 inertial reference.

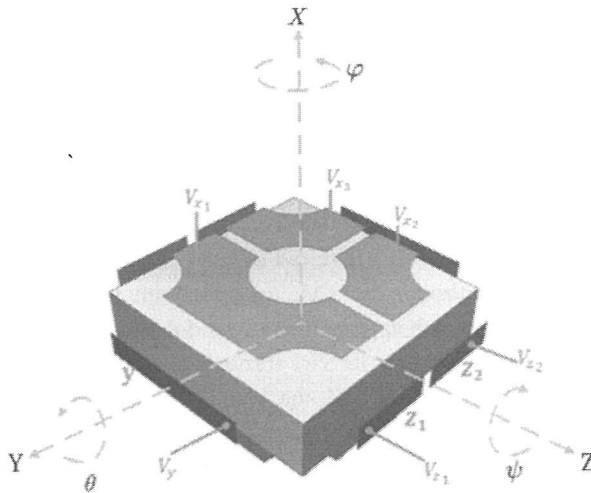


Fig. 5. Electrode layout.

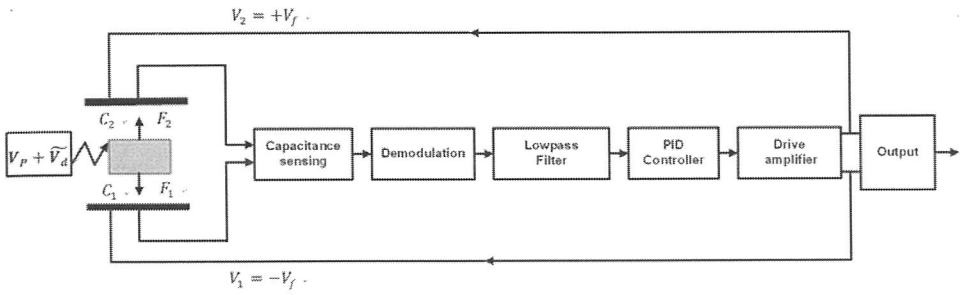


Fig. 6. Measurement principle of inertial reference.

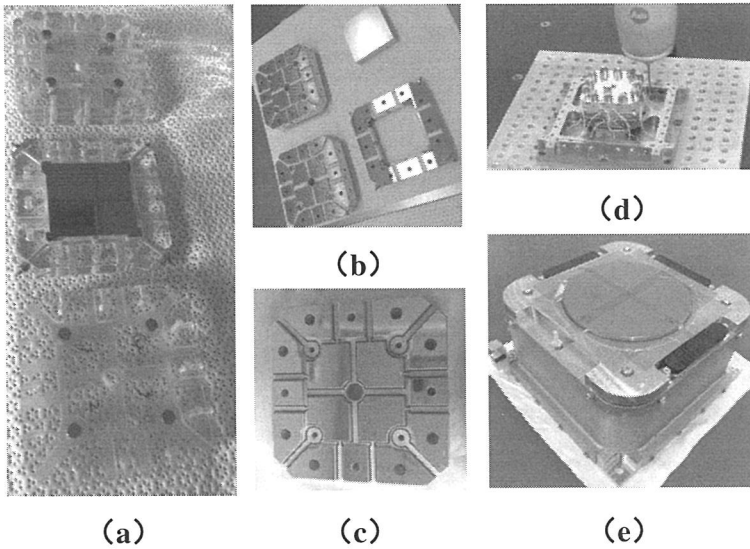


Fig. 7. Sensor fabrication process.

where ϵ_0 is the vacuum dielectric constant, ϵ_r is the relative permittivity, S is the electrode area, d is the average electrode distance, V_f is the feedback control voltage and V_p is the DC bias voltage applied to the TM.

3.4. Fabrication and testing of inertial reference

a. Sensor

As the core of sensitive acceleration signal of Taiji-1 inertial reference, the sensor, to be specific, the accuracy of its processing and assembly, has great influence on the performance of Taiji-1 inertial reference.

First, the ultra-precision machining and optical polishing of the sensor achieves the electrode parallelism and perpendicularity better than $3 \mu\text{m}$, the coplanarity of electrodes on the same side better than $1 \mu\text{m}$ and the electrode flatness better than $1 \mu\text{m}$, all of which meet the design requirements. The machined electrode plate and TM are shown in

Fig. 7(a). Second, the surface metallization of TM and electrode housing is achieved by magnetron sputtering, as shown in Fig. 7(b). Then, the electrodes are fabricated by femtosecond laser etching, as shown in Fig. 7(c). Finally, the precision assembly of this sensor is completed with the aid of CMM to achieve the micron-level assembly accuracy, as shown in Fig. 7(d). The flight model of Taiji-1 inertial reference sensor is shown in Fig. 7(e).

b. Electronics

Electronics is the measurement and control unit of Taiji-1 inertial reference. The differential capacitance between TM and electrode plate is converted into voltage through capacitance sensing circuit to realize the accurate measurement of TM position. In a microgravity environment, a bias voltage can be applied to the electrode plate so that an electrostatic force will be generated between TM and electrode plate to keep the TM stably suspended at the center of the electrode housing.^{9,11,12}

Sensing.

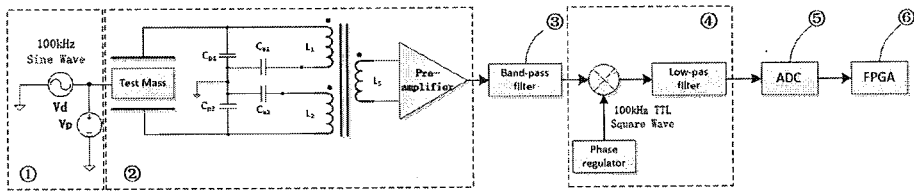


Fig. 8. TM position readout circuit.

The capacitive displacement sensing circuit is mainly composed of a V_d+V_p sinusoidal carrier and DC bias voltage circuit, a capacitance bridge sensing circuit, a preamplifier circuit, a band-pass filter circuit, a phase-sensitive demodulator circuit (with low-pass filter), an Analog to Digital Converter (ADC) circuit and a FPGA controller circuit.

When an acceleration signal is input from outside, the TM will deviate from the center of electrode to generate a differential capacitance, which will then be modulated by 100 kHz carrier signal into an 100 kHz amplitude modulation signal. After being amplified by the capacitance bridge sensing circuit composed of a differential transformer and a preamplifier, the amplitude modulation signal enters the band-pass filter circuit to further filter out its two-sided out-of-band noise and to improve the noise suppression ability of the later-stage phase-sensitive demodulator circuit. Then the phase-sensitive demodulator demodulates the slowly varying differential capacitance signal from the amplitude modulation signal. After low-pass filtering, the differential capacitance signal enters the ADC circuit with a 24-bit Σ - Δ ADC. Finally, the FPGA controller circuit realizes the acquisition and processing of each signal and the calculation of digital PID controller.

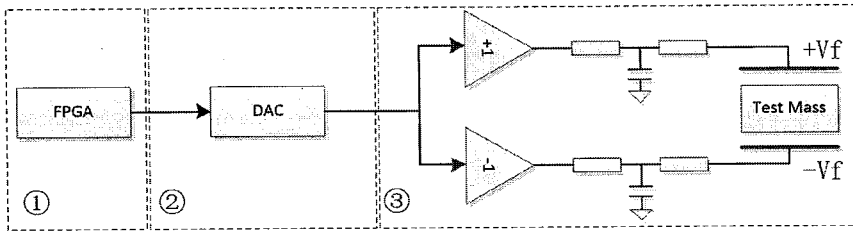
Forcing:

Fig. 9. TM forcing circuit.

The feedback forcing circuit is mainly composed of a FPGA controller circuit, a Digital to Analog Converter (DAC) circuit and a positive and negative forcing circuit. After PID operation, the FPGA controller outputs the differential capacitance displacement signal to a 20-bit DAC and then amplifies the converted analog quantity through forward following amplification and reverse proportional amplification. Through the T -type resistance capacitance filter circuit, the electrostatic feedback control voltage is applied to the corresponding positive and negative plates to generate an electrostatic force that can keep TM near the center of the electrode housing.

4. Ground Test**4.1. Gravity component method**

Before launching, the function and performance of inertial reference were tested and evaluated with gravity component method, torsion pendulum method and free fall method.

After the fabrication of inertial reference was completed, the TM suspension test was realized by improving the feedback control voltage to provide enough electrostatic force that could overcome the influence of gravity. The test was carried out in a quiet cave laboratory. The range, scale factor and other parameters of the inertial reference were tested and calibrated with the gravity component method, as shown in Fig. 10. In order to facilitate the test operation, the bias voltage and maximum feedback control voltage of the designed inertial reference were amplified from 5 and 10 V to 55 and 35 V, respectively, so that the range of the inertial reference was enlarged by nearly 40 times. The calibration curve is shown in Fig. 11. Thus, the scale factor and range of the inertial reference under on-orbit parametric conditions can be deduced. At the same time, the long-term static test of the inertial reference was carried out in the cave laboratory. The spectrum of test noise is shown in Fig. 12. The noise shown in the figure is mainly the coupling result of environmental vibration noise and high-pressure suspension noise, rather than the background test noise of the equipment. This test only proves that the inertial reference can realize long-term servo stability on orbit.

4.2. Torsion pendulum method

A set of semi-physical simulation system based on torsion pendulum was specially developed to verify and evaluate the function and performance of inertial reference before the launch. The noise source of Taiji-1 inertial reference was studied by comparing this system with the semi-physical simulation system on ground in the on-orbit test of inertial reference.¹¹

The material, size, interval and machining accuracy of inertial reference in the semi-physical simulation system based on torsion pendulum are consistent with those of Taiji-1 inertial reference, as shown in Fig. 13(a). The differential capacitance formed by the upper and lower electrodes is a sensitive axis, namely the drag-free control direction of

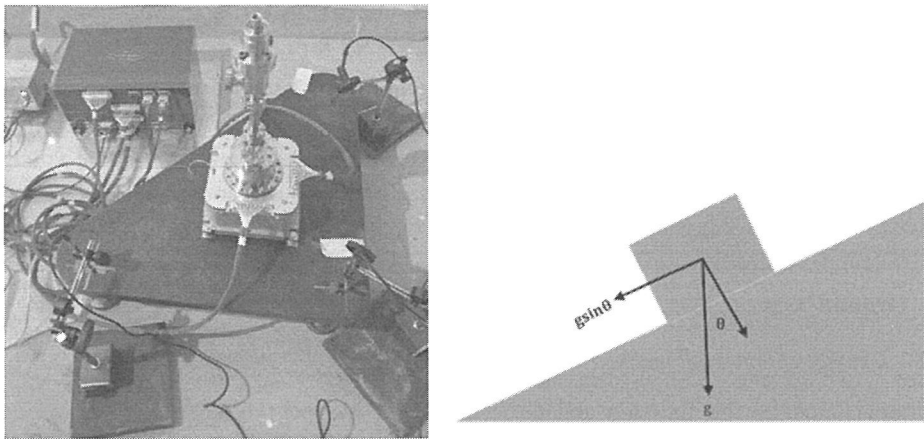


Fig. 10. Ground calibration of inertial reference based on gravity component method.

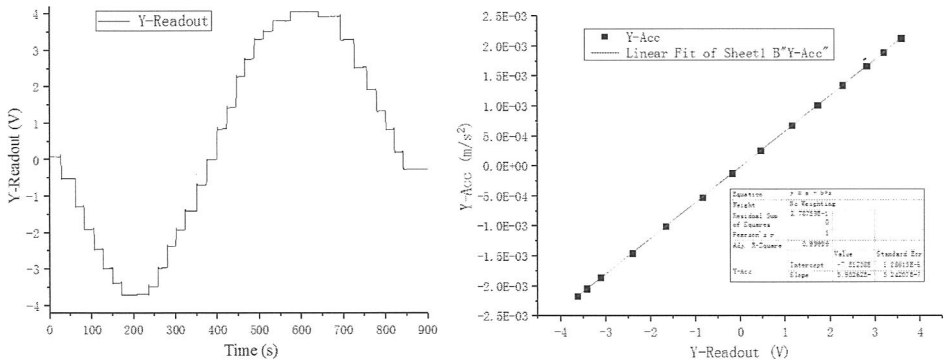


Fig. 11. Calibration test of inertial reference in cave laboratory based on gravity component method.

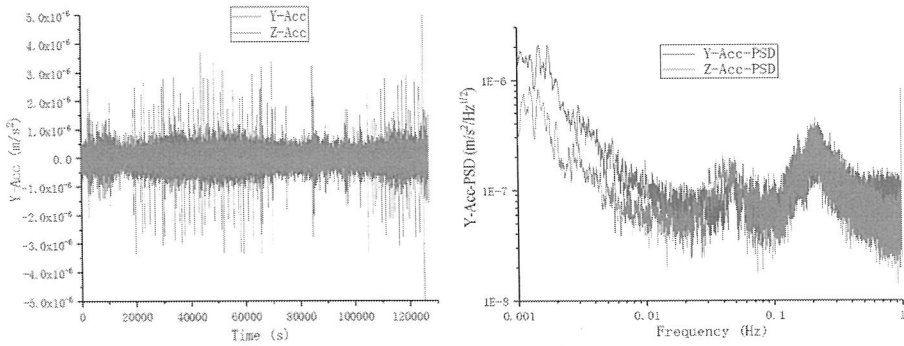
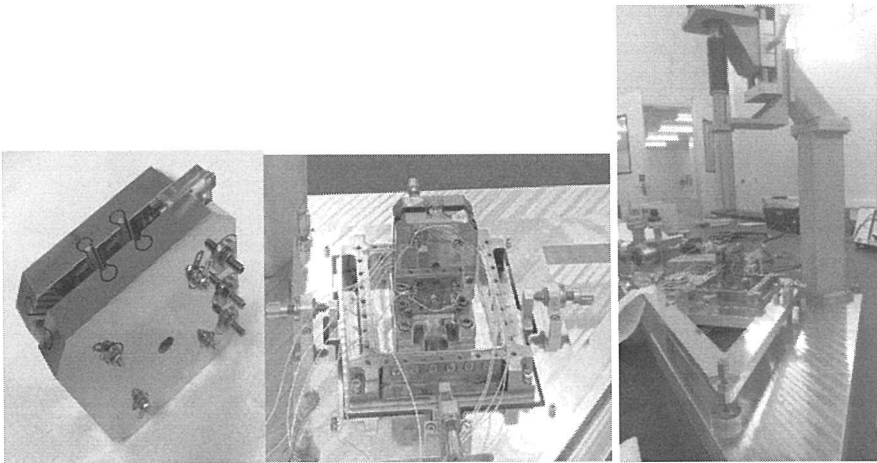


Fig. 12. Time-domain and frequency-domain noise of inertial reference during long-term static test in cave laboratory.



(a) Testing sensor.

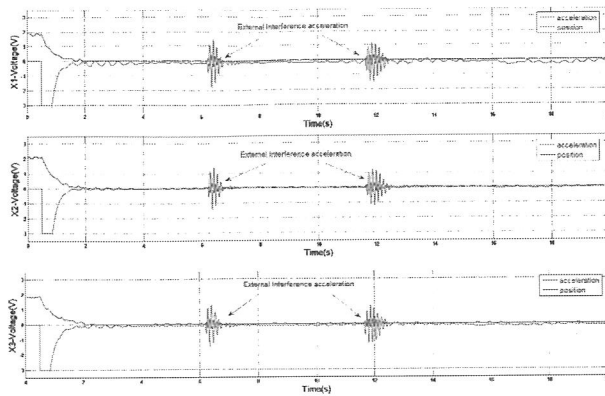
(b) Torsion pendulum.

Fig. 13. Inertial reference for torsion pendulum test.

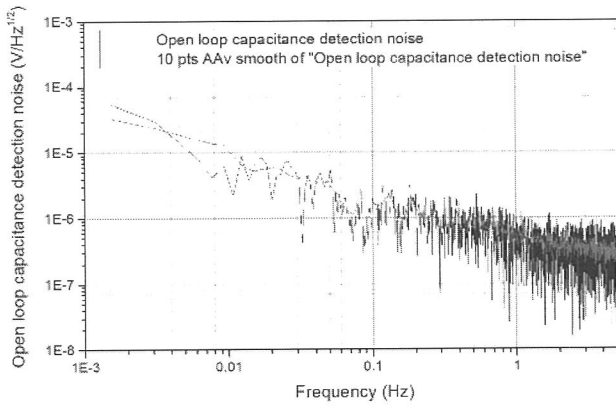
Taiji-1. One TM corresponds to three electrode pairs. Three sensitive axes can realize the 3-DOF acceleration measurement.

As shown in Fig. 13(b), the semi-physical simulation system based on torsion pendulum was built to test the performance indexes of gravitational reference electronics,^{13,14} including 3-DOF closed-loop control stability, range, electricity-force conversion factor and closed-loop acceleration resolution.

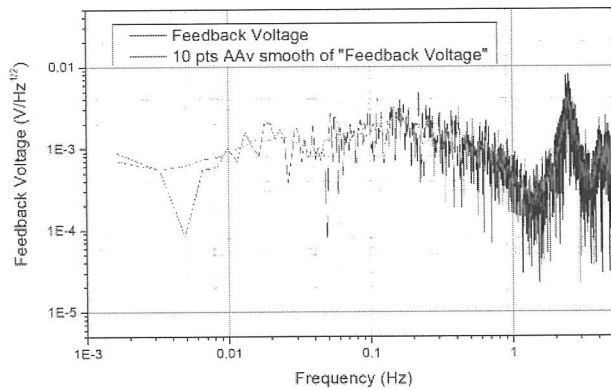
The range of the system is $-6.7 \times 10^{-3} \text{m/s}^2$ to $7 \times 10^{-3} \text{m/s}^2$, and the electric force conversion coefficient is $4.8 \times 10^{-3} \text{m/s}^2/\text{V}$. Finally, the current acceleration noise results of inertial sensors are given. The results show that under current ground conditions, the measured acceleration resolution is only $9.6 \times 10^{-6} \text{m/s}^2$ due to environmental vibration. If the ground wants to measure high indicators, then a cave or



(a) 3-DOF control performance.



(b) Noise of open-loop capacitance sensing circuit.



(c) Noise of closed-loop actuation voltage.

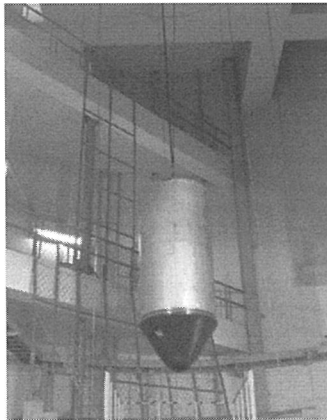
Fig. 14. Results of torsion pendulum test.

underground laboratory must be established to suppress the interference of low-frequency noise on the ground. For this system, if the ambient vibration is not considered, the total acceleration resolution can reach $3.4 \times 10^{-9} \text{ms}^{-2}/\sqrt{\text{Hz}}$.

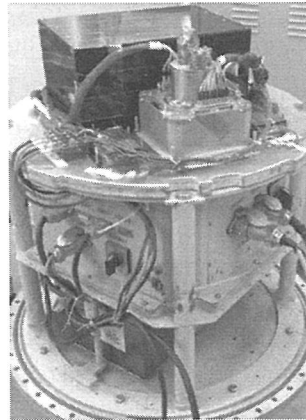
4.3. Free fall test

The free fall test¹² under ground conditions was carried out to demonstrate the rationality of on-orbit sensing and controlling parameters of inertial reference and to verify whether the capture and stable servo control of TM could be realized under on-orbit conditions.

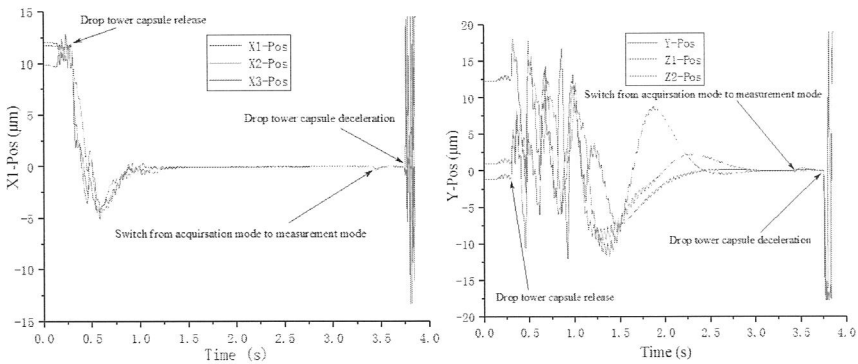
The test was done in the falling tower of the Institute of Mechanics, Chinese Academy of Sciences. The falling tower provided about 3.5 s free-falling time. During this period, the TM of inertial reference was captured in three axial directions after being released in the drop capsule for about 3.2 s, and then successfully switched to the measurement mode, as shown in Fig. 15(c).



(a) Drop capsule

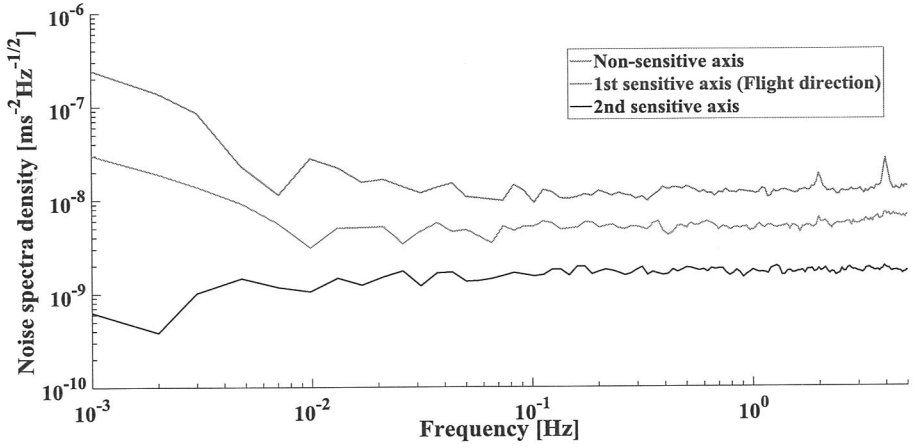


(b) Inertial reference for free fall test

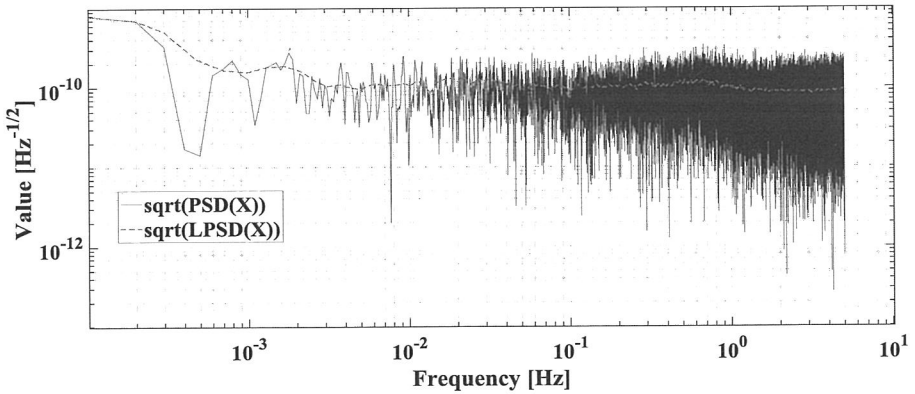


(c) Results of free fall test

Fig.15. Position sensing curve of TM in free fall test



(a)



(b)

Fig. 16. Test results of inertial reference on orbit. (a) Accelerations of Taiji-1 S/C in three axes, as read out by inertial reference and (b) Noise of Taiji-1 inertial reference.

4.4. Test results of inertial reference on orbit

The noise of inertial reference was sampled from the second sensitive axis. The dynamic range of the second sensitive axis was $\pm 5.3 \times 10^{-5} \text{ ms}^{-2}$, and the acceleration noise of this axis measured from the readout voltage fluctuation was $10^{-10} \text{ ms}^{-2}/\text{Hz}^{1/2}$ (Fig. 16(a)). The noise of inertial reference induced by voltage fluctuation is always proportional to its dynamic range (see Eq. (5)). In the equation, S is the area of the capacitor plate, m is the mass of TM, d is the capacitor distance, V_p is the preloaded voltage of the capacitor, V_r is the readout voltage, δV_p is the noise of preloaded voltage, δV_r is the noise of readout

voltage and ϵ_0 is Electrostatic constant.

$$\text{Readout acceleration: } A_{\text{readout}} = \frac{2\epsilon_0 S}{md^2} V_p V_r, \quad (2)$$

$$\text{Acceleration noise: } \delta a = \frac{2\epsilon_0 S}{md^2} V_p V_r \left(\frac{\delta V_p}{V_p} + \frac{\delta V_r}{V_r} \right). \quad (3)$$

So, the acceleration noise will decrease with the dynamic range (see Fig. 16(a)). The disturbance accelerations in the three axial directions of Taiji-1 S/C read out by Taiji-1 inertial reference is given in Fig. 16(b). The nonsensitive axis is Earth-pointing, where the noise is mainly dominated by readout noise. The first sensitive axis is along the flight direction, where the noise is mainly contributed by air drag. The second sensitive axis is along the normal direction of orbit plane, where the acceleration measured by inertial reference is below $2 \times 10^{-9} \text{ ms}^{-2}/\text{Hz}^{1/2}$.

5. Conclusion

The successful test of the Taiji-1 inertial reference has verified that sensor built, sensing and forcing electronics scheme are feasible. With further experiments on orbit and on ground, we will have a deeper understanding of inertial reference performance and noise sources. Encouraged by the achievement of Taiji-1, the inertial reference required by the Taiji Program ($3 \times 10^{-15} \text{ ms}^{-2}/\sqrt{\text{Hz}}$) will be built in near future, and the Taiji scientific collaboration is looking forward to flying Taiji in early 2030s.

Acknowledgments

This work is supported by the ‘‘Strategic Priority Research Program of the Chinese Academy of Science’’ (XDA15020709, XDB23030000) and ‘‘Foreign Key Projects of International Cooperation’’ (181722KYSB20190040). Zhi Wang and Jun-Gang Lei equally contribute to this work.

References

1. W. Fichter, P. Gath, S. Vitale and D. Bortoluzzi, *Class. Quantum Grav.* **22**, S139 (2005).
2. D. Mance, Development of electronic system for sensing and actuation of test mass of the inertial sensor LISA, FESB & ETH (2012).
3. D. Cyranoski, *Nat. News* **531**, 150 (2016).
4. W. R. Hu and Y. L. Wu, *Natl. Sci. Rev.* **4**, 685 (2017).
5. Z. R. Luo, Z. K. Guo, G. Jin, Y. L. Wu and W. R. Hu, *Results Phys.* **16**, 102918 (2020).
6. M. Armano, H. Audley, G. Auger, J. T. Baird, M. Bassan, P. Binetruy, M. Born, D. Bortoluzzi, N. Brandt, M. Caleno, L. Carbone, A. Cavalleri, A. Cesarini, G. Ciani, G. Congedo, A. M. Cruise, K. Danzmann, M. de Deus Silva, R. De Rosa, M. Diaz-Aguil’o, L. Di Fiore, I. Diepholz, G. Dixon, R. Dolesi, N. Dunbar, L. Ferraioli, V. Ferroni, W. Fichter, E. D. Fitzsimons, R. Flatscher, M. Freschi, A. F. García Marín, C. García Marirrodriga, R. Gerndt, L. Gesa, F. Gibert, D. Giardino, R. Giusteri, F. Guzmán, A. Grado, C. Grmani, A. Grynagier, J. Grzymisch, I. Harrison, G. Heinzel, M. Hewitson, D. Hollington, D. Hoyland, M. Hueller, H. Inchauspé, O. Jennrich, P. Jetzer, U. Johann, B. Johlander, N. Karnesis, B. Kaune, N. Korsakova, C. J. Killow, J. A. Lobo, I. Lloro, L. Liu, J. P. López-Zaragoza, R.

- Maarschalkerweerd, D. Mance, V. Martín, L. Martin-Polo, J. Martino, F. Martin-Porqueras, S. Madden, I. Mateos, P. W. McNamara, J. Mendes, L. Mendes, A. Monsky, D. Nicolodi, M. Nofrarias, S. Paczkowski, M. Perreur-Lloyd, A. Petiteau, P. Pivato, E. Plagnol, P. Prat, U. Ragnit, B. Raïs, J. Ramos-Castro, J. Reiche, D. I. Robertson, H. Rozemeijer, F. Rivas, G. Russano, J. Sanjuán, P. Sarra, A. Schleicher, D. Shaul, J. Slutsky, C. F. Sopena, R. Stanga, F. Steier, T. Sumner, D. Texier, J. I. Thorpe, C. Trenkel, M. Tröbs, H. B. Tu, D. Vetrugno, S. Vitale, V. Wand, G. Wanner, H. Ward, C. Warren, P. J. Wass, D. Wealthy, W. J. Weber, L. Wissel, A. Wittchen, A. Zambotti, C. Zanoni, T. Ziegler and P. Zweifel, *Phys. Rev. Lett.* **116**, 231101 (2016).
7. E. A. Heather, IOP Conf. Ser.: *J. Phys.: Conf. Ser.* **840**, 012034 (2017).
 8. P. Touboul, E. Willemonot, B. Foulon and V. Josselin, *Boll. Geofis. Teor. Appl.* **40**, 321 (1999).
 9. D. Lauben, G. Allen, W. Bencze, S. Buchman, R. Byer, A. Goh, S. Dorlybounxou, J. Hanson, L. Ho, S. Higuchi, G. Huffman, F. Sabur, K. Sun, R. Tavernetti, L. Rolih, R. Van Patten, J. Wallace and S. Williams, *AIP Conf. Proc.* **873**, 576 (2006).
 10. B. Frommknecht, U. Fackler and J. Flury, Integrated sensor analysis of the GRACE Mission, Universität München (2007).
 11. Y. Wang, K. Qi, S. Wang, W. Li, Z. Li and Z. Wang, *IEEE Access* **8**, 1021 (2020).
 12. J.-P. Marque, B. Christophe, F. Liorzou, G. Bodoville, B. Foulon, J. Guerard and V. Lebat, The ultra sensitive accelerometers of the ESA GOCE mission, in 59th Int. Astronautical Congress, 29 Septembre–3 Octobre 2008.
 13. G. Ciani, A. Chilton, S. Apple, T. Olatunde, M. Aitken, G. Mueller and J. W. Conklin, *Rev. Sci. Instrum.* **88**, 064502 (2017).
 14. D. Nicolodi, Toward a third generation torsion pendulum for the Femto Newton level testing of free fall in the laboratory, University of Trento, 2006–2007.